

available at [www.sciencedirect.com](http://www.sciencedirect.com)[www.elsevier.com/locate/brainres](http://www.elsevier.com/locate/brainres)**BRAIN  
RESEARCH****Research Report****Long-term cognitive impairment and myelination deficiency in a rat model of perinatal hypoxic-ischemic brain injury**Zhiheng Huang<sup>a,b</sup>, Jiangqin Liu<sup>a,b</sup>, Po-Yin Cheung<sup>c</sup>, Chao Chen<sup>a,b,\*</sup><sup>a</sup>Department of Neonatology, Children's Hospital of Fudan University, Shanghai, China<sup>b</sup>Key Laboratory of Neonatal Disease, Ministry of Health, Shanghai, China<sup>c</sup>Department of Pediatrics, University of Alberta, Edmonton, Canada

## ARTICLE INFO

## Article history:

Accepted 3 September 2009

## Keywords:

Hypoxia-ischemia

Myelination

Cognitive function

Newborn

Rat

## ABSTRACT

Although periventricular white matter injury is a leading cause of major neurologic disability in premature infants, the relationship between myelination deficiency and long-term cognitive dysfunction is not well understood. The purpose of this study was to investigate oligodendrocytes myelination and long-term spatial cognitive function in rats with perinatal hypoxia-ischemia (HI). Postnatal day 3 (P3) rats were subjected to right carotid artery ligation followed by 2.5 h of hypoxia (6% oxygen). Brain injury during the early and late phases was evaluated by immunostaining at P6 (72 h after the injury) and P47. Spatial cognitive function was evaluated at P42 using the Morris Water Maze test followed by histologic evaluation. HI caused an increase in pre-oligodendrocytes, astrocytes, and microglia in the ipsilateral white matter 72 h after the insult compared to contralateral regions and sham-operated controls (both  $p < 0.05$ ). There were significant decreases in myelin basic protein (MBP) and 2',3'-cyclic nucleotide 3'-phosphodiesterase (CNPase)-labeled oligodendrocytes with glial fibrillary acidic protein (GFAP)-labeled glial scarring in the ipsilateral periventricular white matter at P47 compared to contralateral regions and sham-operated controls (all  $p < 0.05$ ). The rats with HI had spatial learning deficits in navigation trials (longer escape latency and swimming distance) and memory dysfunction in probe trials (fewer number of platform crossings and percentage of time in the target quadrant) compared with sham-operated controls ( $p < 0.05$ ). In this neonatal rat model of HI, myelination deficiency induced by activated astrocytes and microglia during the early phase with subsequent glial scarring was associated with long-term spatial learning and memory dysfunction.

© 2009 Elsevier B.V. All rights reserved.

**1. Introduction**

Although the mortality of premature infants with gestation less than 32 weeks has decreased significantly over the last two decades, the incidence of periventricular white matter injury (PWMI) remains very high in survivors (Volpe, 2001). These survivors have a high incidence of long-term neurologic

disabilities, including cerebral palsy (5%–15%) and cognitive disabilities (30%–50%) (Marlow et al., 2005; Taylor et al., 2004). Pathogenic mechanisms of PWMI include immature penetrating vasculature, deficiency of cerebrovascular autoregulation, and vulnerability of late oligodendrocyte progenitors (preOLs) (Back and Volpe, 1997; Back et al., 2002). PreOLs, which are the progenitors of myelinating cells, are targets of hypoxic-ischemic

\* Corresponding author. Fax: +86 21 64931916.

E-mail address: [chen6010@163.com](mailto:chen6010@163.com) (C. Chen).

(HI) insults during the perinatal period. The loss of myelination and/or dysmyelination of OLS is a key feature of PWMI in premature infants. To date, numerous studies have focused on the role of neurons in cognitive function after perinatal HI insults (Ten et al., 2003); however, the role of myelin has not been equally investigated.

The period of greatest susceptibility for PWMI is between 23 and 32 weeks gestation. The definition of PWMI has changed through the years, initially described as severe focal cystic lesions but now including focal or diffuse noncystic lesions (Back, 2006). In an established model of moderate brain injury using postnatal 3 day (P3) rat pups, the age at which the development of OLS in the neonatal rat brain is similar to that of premature human infants between 23 and 32 weeks gestation (Craig et al., 2003), we investigated the relationship between dysmyelination and long-term cognitive function of rats after neonatal HI. Our hypothesis was that myelination deficiency, induced by mechanisms in both the early (72 h after insult, or P6) and late phases (44 days after insult, or P47) after the HI insults, is associated with long-term cognitive impairment.

## 2. Results

### 2.1. Expression of preOLs, astrocytes, and microglia in the early phase (72 h) after HI

O4 antibody specific for sulfatides on preOL cell membranes was used to label preOLs. An abundance of O4<sup>+</sup> preOLs was detected in the cingulum, subcortical white matter, and corpus callosum of the rat brain 72 h after HI insult. The number of O4<sup>+</sup> preOLs was significantly higher in the ipsilateral white matter than in the corresponding contralateral regions and sham-operated controls (35±5 cells/hpf vs. 21±1 cells/hpf and 15±1 cells/hpf, respectively;  $p < 0.05$ ; Figs. 1A–C).

Glial fibrillary acidic protein (GFAP) immunostaining was performed on P6 to evaluate astrogliosis. HI insult induced astrogliosis, characterized by glial hypertrophy and hyperplasia. Reactive astrogliosis was most evident in the subcortical white matter, especially the cingulum and corpus callosum of the ipsilateral white matter, and was quantitative greater than that in the corresponding contralateral regions and sham-operated controls (83±7 cells/hpf vs. 40±4 cells/hpf and 32±2 cells/hpf, respectively;  $p < 0.01$ ; Figs. 1D–F).

CD68 immunostaining was performed to evaluate activated microglia–macrophages. HI was associated with a significantly increased number of CD68<sup>+</sup> microglia in the ipsilateral white matter compared with the contralateral side and sham-operated control group (56±4 cells/hpf vs. 35±6 cells/hpf and 23±3 cells/hpf, respectively;  $p < 0.05$ ; Figs. 1G–I). In control rat brains, amoeboid microglia were identified in the susceptible periventricular region; resting-state microglia were detected in other regions with similar distribution patterns of astrocytes.

### 2.2. Expression of OLS, glial scar, microglia, and neurons in the late phase (44 days) after HI

To further evaluate the long-term recovery of preOLs after HI insult, we assessed myelin expression with myelin basic protein (MBP) immunostaining in the brain of P47 rats. The brains of the

sham-operated control group had a normal myelination pattern. Weak MBP immunostaining was found in the ipsilateral subcortical white matter and corpus callosum but not in the contralateral regions of HI rats (Figs. 2A–C). A significant decrease in the MBP-immunostained area was observed in the ipsilateral white matter of P47 rats after HI; there was no such decrease noted in the HI contralateral regions and sham-operated controls (2.5±0.2 mm<sup>2</sup> vs. 3.8±0.2 mm<sup>2</sup> and 4.0±0.3 mm<sup>2</sup>, respectively;  $p < 0.05$ ). Furthermore, in the white matter the projection fibers were hypomyelinated by HI, twisted (Fig. 2D), and decreased connection in the neocortex (Fig. 2A); this phenomenon was not found on the HI contralateral regions and control group (Figs. 2B, E and C, F). There were also less 2',3'-cyclic nucleotide 3'-phosphodiesterase (CNPase)-positive cells (stained soma of OLS) in the ipsilateral white matter compared to corresponding HI contralateral regions and sham-operated controls (14±2 cells/hpf vs. 25±2 cells/hpf and 31±3 cells/hpf of the contralateral region and sham-operated controls, respectively;  $p < 0.05$ ; Figs. 2G–I). These findings suggest that both the myelin and soma of OLS were decreased 44 days after HI injury.

GFAP is a marker for glial scarring (Di Giovanni et al., 2005; Zhu et al., 2007b), a process which is deleterious to normal myelination (Fawcett and Asher, 1999). In the ipsilateral white matter of P47 rats, GFAP-labeled glial scarring was greater in HI sites than in the contralateral region and sham-operated controls (47±6 cells/hpf vs. 26±2 cells/hpf and 23±3 cells/hpf, respectively; all  $p < 0.05$ ; Figs. 2J–L). However, the expression of CD68<sup>+</sup> microglia was not significantly elevated in the ipsilateral white matter, contralateral region, or sham-operated controls and nearly all of the microglia cells were in the resting state (data not shown).

Nissl and NeuN staining was used to identify neurons and assess neuronal damage (Fan et al., 2008b; Ten et al., 2003). Because the CA1 region of the hippocampus plays a key role in spatial cognitive function, the expression of neurons from three separate fields in this region was selected for Nissl and NeuN staining. As expected, HI reduced the number of neurons in the ipsilateral CA1 region compared with the contralateral part and control group (80.7±2.6 cells/hpf vs. 97.0±3.7 cells/hpf and 99.0±2.4 cells/hpf, respectively;  $p < 0.05$ ; Figs. 3A–C). Nissl staining data were confirmed by NeuN immunostaining, which detects the nuclei of neurons with slight cytoplasmic staining. As expected, the number of NeuN-positive cells in the ipsilateral CA1 region was decreased compared with the contralateral region and control group (81.2±4.4 cells/hpf vs. 97.6±3.5 cells/hpf and 98.4±3.7 cells/hpf, respectively;  $p < 0.05$ ; Figs. 3D–F).

### 2.3. Histologic analysis on P47

The cerebral hemisphere of P47 rats in the sham-operated control group showed histologic integrity with cresyl violet staining (Figs. 4A and D). However, the corpus callosum was thinner and brain atrophy with and without partial tissue loss was observed in the ipsilateral hemisphere (Figs. 4B, C, E, and F). Compared to contralateral and sham-operated controls, there were significant reductions in the ipsilateral corpus callosum area ([R:L]<sub>AREA</sub>: 0.75±0.04 vs. 1.01±0.01 of HI rats and sham-operated controls, respectively;  $p < 0.05$ ; Fig. 4G.) and the volume of the HI-insulted hemisphere ([R:L]<sub>AREA</sub>: 0.81±0.05 vs. 0.96±0.01 of the sham-operated controls;  $p < 0.05$ ; Fig. 4H).

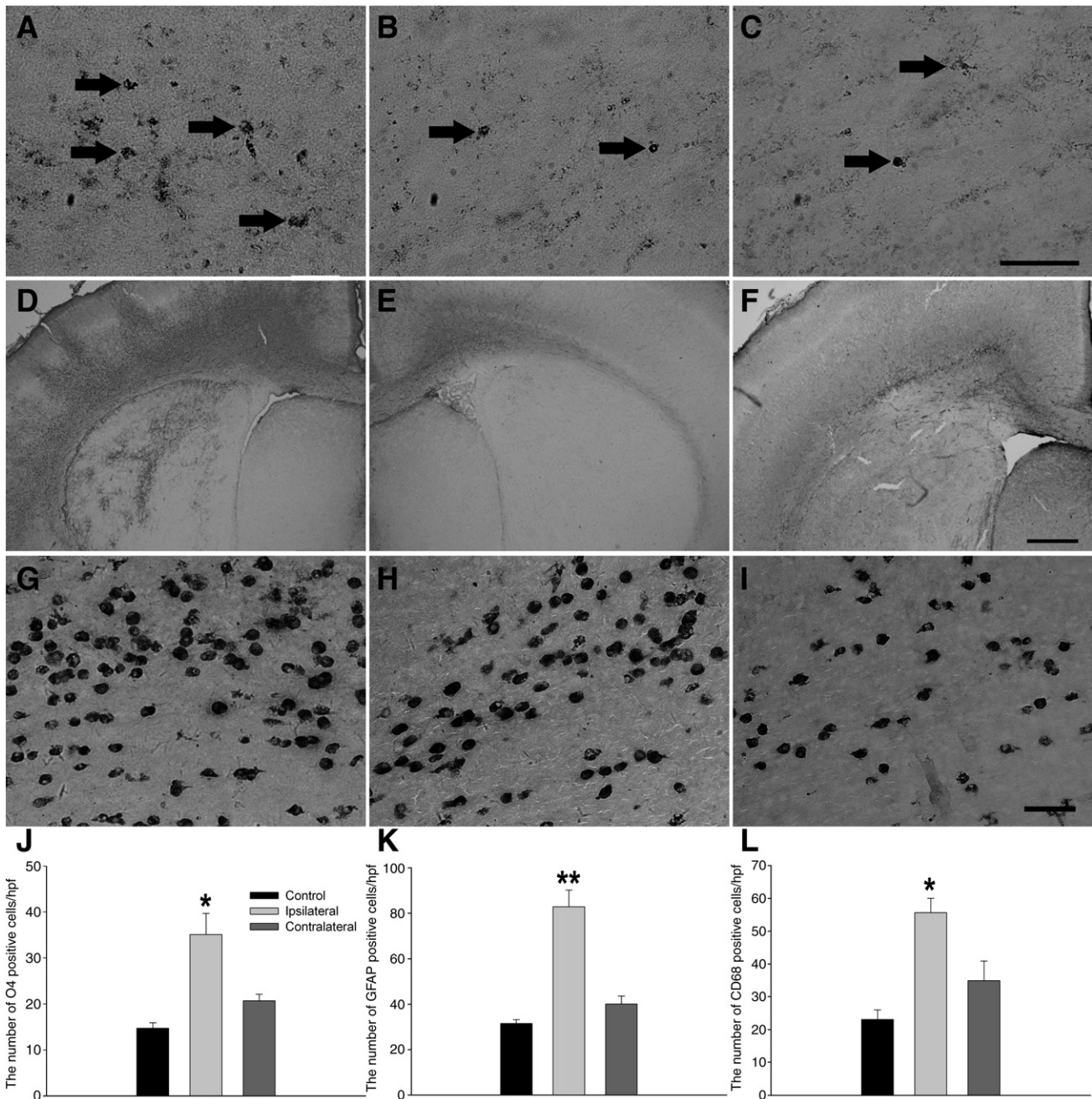


**Fig. 1** – Representative photomicrographs of O4, GFAP, and CD68 immunostaining and cell counting at 72 h after HI. The number of O4-, GFAP-, and CD68-positive cells significantly increased in the ipsilateral white matter (A, D, and G, respectively) but not in the corresponding contralateral region (B, E, and H, respectively) or the control group (C, F, and I, respectively). (J–K) Cell counting. Scale bar = 50  $\mu$ m (A–C and G–I) and 500  $\mu$ m (D–F). (\* $p$  < 0.05, \*\* $p$  < 0.01).

#### 2.4. Morris water maze test at P42 to P46

In Morris Water Maze navigation trials, the HI group had a significantly longer escape latency ( $p$  < 0.05) and swimming distance ( $p$  < 0.05) than sham-operated control rats from the 1st day to the 4th day of testing (P42–P45; Figs. 5A and B). In water maze probe trials on P46, the HI rats had fewer platform crossings ( $p$  = 0.01) and a lower percentage of time in the target quadrant ( $p$  < 0.05) compared with the sham-operated controls (Figs. 5C and D). However, there was no significant difference in

swimming speed between the HI and sham-operated control groups (210  $\pm$  16 mm/s vs. 225  $\pm$  16 mm/s, respectively;  $p$  = 0.50).

### 3. Discussion

Our data suggest that HI impairs the preOLs myelination process and contributes to astrogliosis and microgliosis during the early phase (72 h after insult) and glial scarring in the late phase (44 days after insult). These findings may be one of the

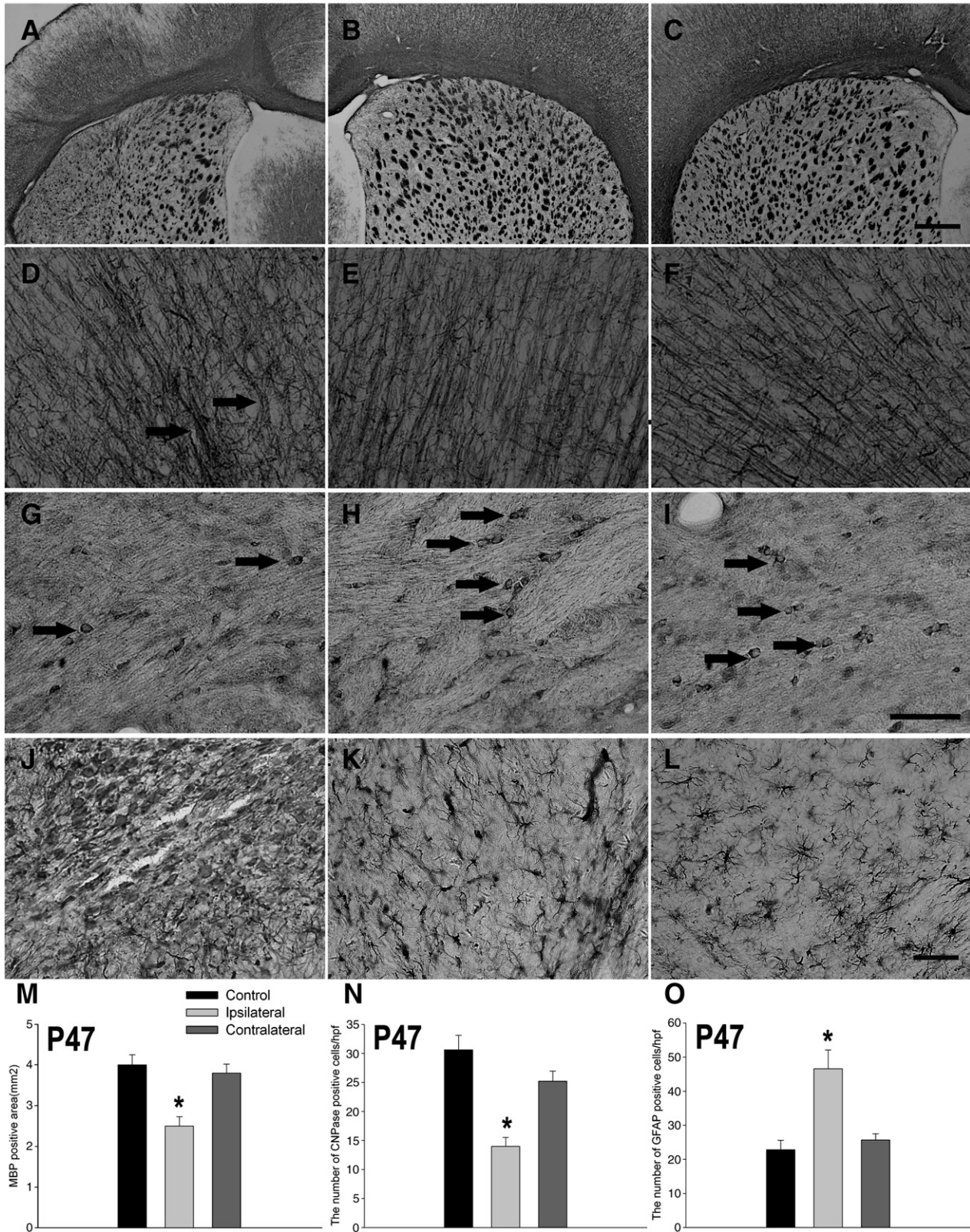


**Fig. 2** – Representative photomicrographs of MBP, CNPase, and GFAP immunostaining and cell counting at P47. HI insults results in myelination deficiency involving twisted projection fibers and a reduction of OLs in the ipsilateral hemisphere (A, D, and G, respectively); these changes were not observed at corresponding levels in the contralateral hemisphere (B, E, and H, respectively) or control group (C, F, and I, respectively). GFAP-labeled glial scarring was sustained in the ipsilateral white matter compared with the contralateral white matter and control group (J, K, and L, respectively). (M–O) Cell counting. Scale bar = 500  $\mu$ m (A–C) and 50  $\mu$ m (D–O) (\* $p$  < 0.05).

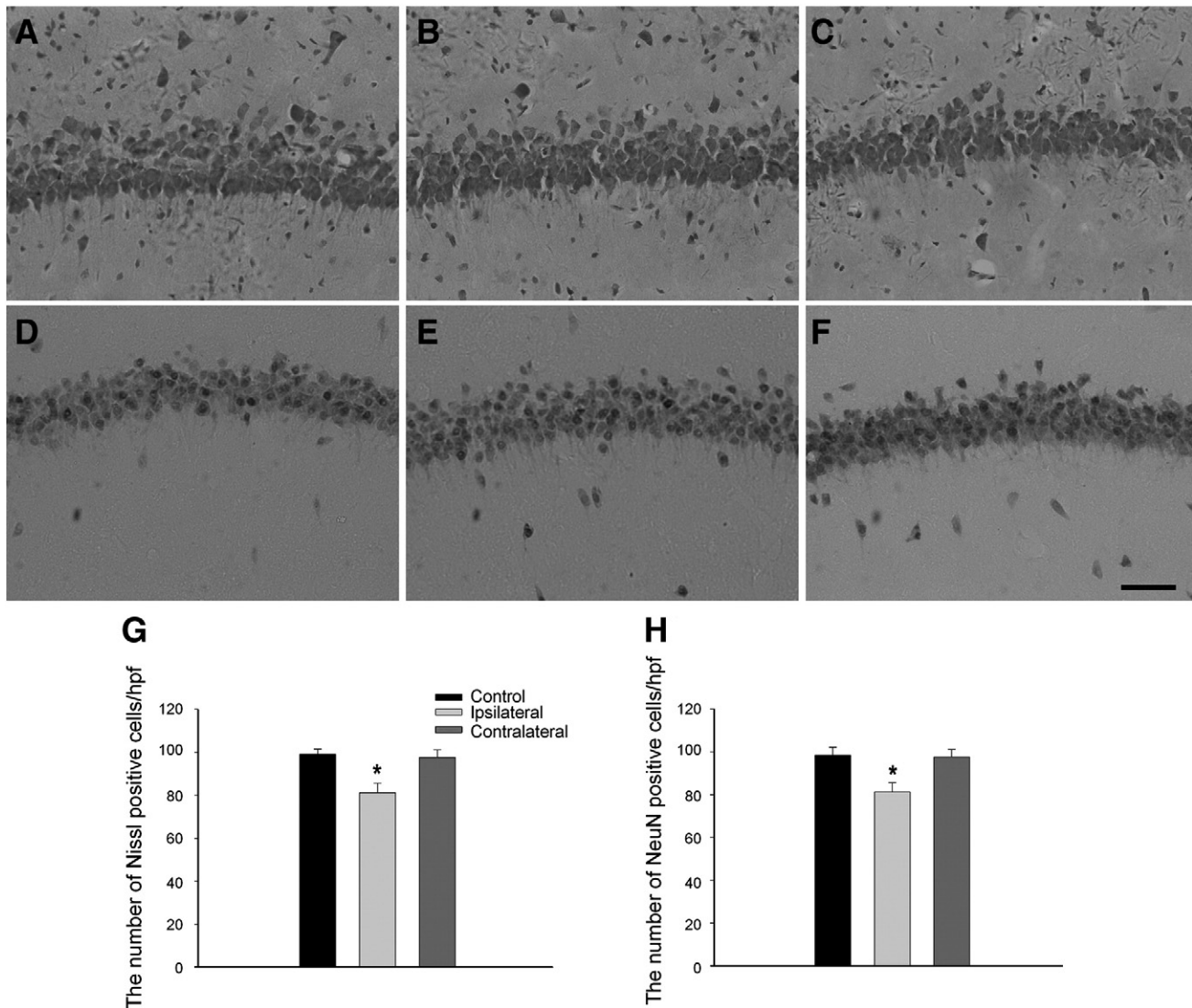


**Fig. 3 – Representative photomicrographs of Nissl and NeuN staining and cell counting in the CA1 region of P47 rat brains. HI reduced the number of Nissl-stained neuronal cells in the CA1 region of the ipsilateral hippocampus (A) compared with the corresponding contralateral region and control group (B and C, respectively). NeuN staining showed similar results in the CA1 region of the ipsilateral hippocampus (D) compared with the contralateral part and control group (E, F). (G–H) Cell counting. Scale bar = 50  $\mu$ m. (\* $p$  < 0.05).**

cellular mechanisms of long-term cognitive dysfunction, including spatial learning and memory deficits in rats with perinatal HI.

HI injury in the full-term brain is characterized by significant neocortical and subcortical neuronal cell damage (Zhu et al., 2007a). However, HI injury in the premature brain is characterized by selective white matter damage and myelination deficiency with relative cortical sparing (Cai et al., 2001; Follett et al., 2000). Myelin abnormalities and deficiencies are known to play important roles in cognitive dysfunction in neurologic diseases such as schizophrenia (Dwork et al., 2007) and multiple sclerosis (Dineen et al., 2009) and are found in irradiated rat brains (Akiyama et al., 2001). While it is known that HI impairs neurologic function and early motor behavior (Lin et al., 2005), the relationship between myelination and later cognitive outcome in the model of perinatal HI is not well

understood, despite it being one of the most important sequelae of extreme prematurity.

The Morris water maze is a standard research tool for assessment of spatial learning and memory is associated with hippocampal cognitive function (Vorhees and Williams, 2006). It has also been used to assess cognition associated with other brain regions involved in spatial cognitive functions (D'Hooge and De Deyn, 2001; Ohta et al., 1997). Our findings from the neonatal rat model of HI showed that HI resulted in spatial learning and memory deficits in P42–P46 rats, corresponding to the age of young adults in humans, similar to that which is observed in school-aged children with perinatal PWMI (Taylor et al., 2004).

Our MBP staining results showed OL myelination deficiency in HI rats, consistent with published reports (Liu et al., 2002). Myelin is responsible not only for protection and

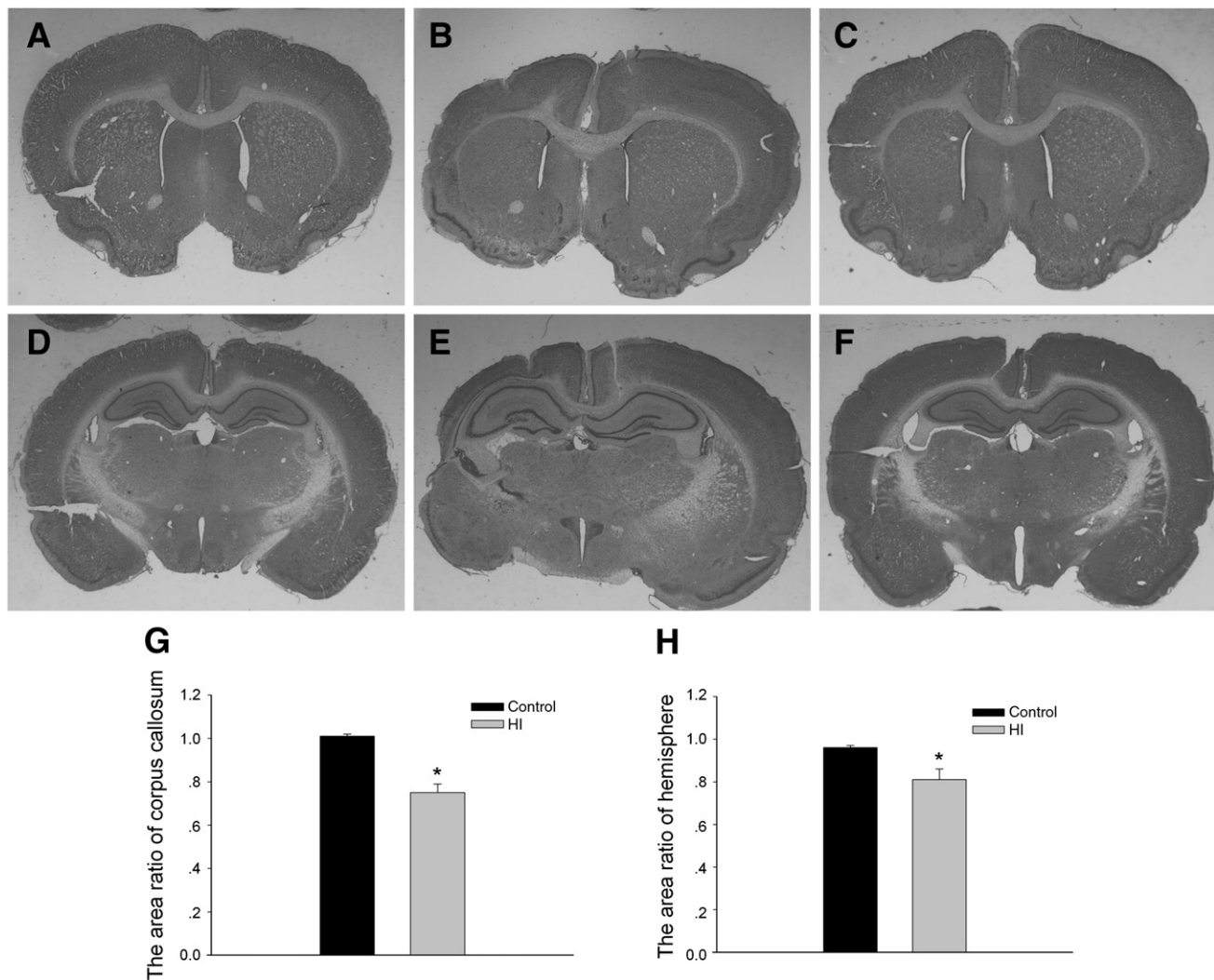


**Fig. 4 – Representative photomicrographs of brain injury and ratio calculation in P47 rats. There were no histologic changes in the control group (A, D) and HI-induced moderate injury with (B, E) or without partial tissue loss (C, F) in the cresyl violet-stained brain. HI induced a decrease in the ratio of (R:L)<sub>AREA</sub> of the corpus callosum and hemisphere (G and H, separately). The right hemisphere was nicked with a razor blade for identification. (\* $p < 0.05$ ).**

insulation of axons but also for production of supportive neurotrophic factors. Thus, loss of myelin will have an adverse effect on axonal function and neuronal survival (Lin et al., 2004). Interestingly, recent studies suggest that myelin may also play an important role in learning and memory function (Fields, 2008a,b; Miki et al., 2009), likely due to its involvement in information processing and conduction velocity regulation. Axonal conduction velocity is regulated by both its diameter and the thickness of the myelin sheath. Thus, myelin sheath abnormalities will adversely influence conduction velocity (Fields, 2008b). Furthermore, myelination deficiency will result in insufficient interconnections of cortical regions involved in information processing. For example, cognitive decline in multiple sclerosis patients has been associated with myelination deficiency and shortened connections between the white and grey matter (Dineen et al., 2009; Kujala et al., 1997). Even if myelin is repaired by endogenous mechanisms, its genes and microstructure may be permanently altered (Skoff et al., 2001),

resulting in diffuse dysfunctional axonal wrapping and inadequate axonal connections. Interestingly, we observed similar findings in our model of perinatal HI injury (Fig. 2D).

In this study, HI resulted in a significant increase of O4<sup>+</sup> preOLs in white matter ipsilateral to the injury 72 h after HI. It is known that HI injury to preOLs occurs via acute caspase-independent and delayed caspase-dependent degeneration mechanisms (Segovia et al., 2008); it is likely that this also would result in long-term myelination deficiencies. HI-mediated preOL cellular death occurs via the excitotoxic and oxidative damage during the acute phase of HI injury (Back, 2006), associated with microglia and astrocyte reactivity. In the early phase of the current study (72 h after HI), we found increases in CD68-labeled microglia and GFAP-labeled astrocytes, both which serve as sources of reactive oxygen and nitrogen species and pro-inflammatory cytokines, such as TNF- $\alpha$  and IL-6 (Cai et al., 2006). This microglia and astrocyte-mediated inflammatory response caused preOLs injury during

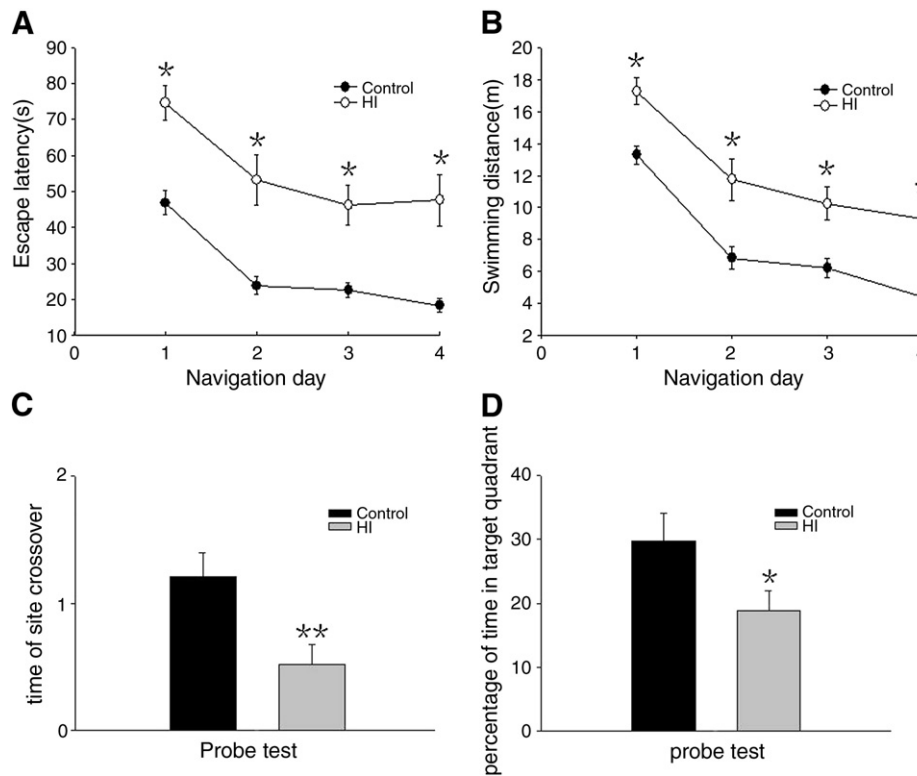


**Fig. 5 – Cognitive function was evaluated by the Morris water maze test on P42. In the navigation trial, a reduction in learning ability was manifested in the HI group as a prolonged escape latency (A) and swimming distance (B) compared with the control group, although improvement did occur with learning. In the space probe trial, a reduction in memory ability was manifested in the HI by fewer platform site crossovers (C) and a lower percentage of time spent in the target quadrant (D). (\* $p < 0.05$ ).**

the early phase, associated with an increase of degenerated preOLs. During the late phase of endogenous recovery (44 days after HI), the number of reactive microglia and astrocytes subsequently declined but the GFAP-labeled glial scar persisted in the lesion sites. Glial scarring is associated with arrest of the normal maturation of preOLs and the subsequent generation of myelin. Our MBP and CNPase immunostaining findings confirmed these results. Although partial astrocyte activity could confer neuroprotection by scavenging reactive oxygen species and assist with reconstruction from brain injury (Sizonenko et al., 2008), excessive astrocyte activity can have deleterious consequences, including the formation of a glial scar. A glial scar may act as a physical barrier blocking growth factor transmission, resulting in preOL myelination deficiencies and neuronal signaling impairment. Furthermore, glial scarring can influence the cell cycle time of preOLs, inhibit preOLs recruited to lesion sites, and decrease its differentiation into mature OLs by secreting multiple inhibitory factors, such as hyaluronic acid (Segovia et al., 2008). The physical barrier of a glial scar may also prevent axons from attaining their full length and arrest new OLs from making axonal contact, both of which will affect normal myelination process and axonal-glial communications (Franklin and Ffrench-Constant, 2008).

In the human brain, myelination is initiated in the third trimester of gestation, a time period during which many preterm infants are in the care of a neonatal intensive care unit and at particularly high risk for PWMI because of preOLs

predominance. Although myelination processes continue through childhood into adolescence and early adulthood, it is associated with a predominance of OLs (Back et al., 2001; Fields, 2005). It is increasingly being recognized that myelination may play an important role in cognitive development; our results are consistent with this hypothesis. Rhesus monkeys or rats fed in enriched environments to encourage an increase in size and number of myelinated axons in the corpus callosum are noted to have improved cognitive function (Juraska and Kopcik, 1988; Sanchez et al., 1998); conversely, our results showed that a decrease in the callosum corpus volume and OLs population may involve cognitive dysfunction in a perinatal HI rat model. Interestingly, Miki et al. (2009) showed a correlation between myelination deficiency and spatial cognitive dysfunction in ischemic white matter mice using adult mice. In summation, these results suggest that myelination deficiency may be associated with cognitive decline.

It has been well known that gray matter injuries are associated with PWMI in premature infants and contribute to cognitive deficits (Inder et al., 2005; Pierson et al., 2007). In particular, the CA1 neurons in the hippocampus are known to play an important role in cognitive function. Furthermore, the fimbria-fornix fibers which are myelinated by the OLs from subventricular zone (Menn et al., 2006) are an important pathway of hippocampocortical connections involved in spatial cognition (D'Hooge and De Deyn, 2001). We detected reductions in the number of CA1 hippocampal neurons in the ipsilateral PWMI hemisphere of P47 rat brains after perinatal

HI. Another study recently reported similar findings of chronic myelination deficiency in the fimbria-fornix in a similar model induced by HI (Stone et al., 2008).

In conclusion, results from our perinatal HI rat model suggest that oligodendrocyte myelination deficiency may be involved in long-term spatial cognitive impairment. Astrogliosis and microgliosis in the early phase within 72 h of the injury and glial scarring in late phase 44 days after the injury may contribute to this phenomenon.

## 4. Experimental procedures

### 4.1. Animal protocols

This study was approved by the Animal Ethics Committee of Fudan University. The perinatal rat model of HI was performed as previously described (Back et al., 2002; Sheldon et al., 1996; Vannucci et al., 1999), with minor modifications. Briefly, after P3 Sprague–Dawley rats were anesthetized with ether, the right common carotid artery was cut between double ligatures. The total time of surgery never exceeded 5 min and any pups with bleeding or respiratory failure were excluded. After surgery, the pups were allowed to recover for 1–1.5 h. The rat pups were then placed in a humidified container maintained at 37 °C. HI was induced by perfusing the container with humidified 6% oxygen in nitrogen gas mixture for 2.5 h. After hypoxic exposure, the pups were returned to their biological dams until they were euthanized per protocol. This resulted in moderate brain injury in the current study. Sham-operated rat pups were randomly chosen from the same litters of HI rats and had neither common carotid artery ligation nor a period of hypoxia.

### 4.2. Immunostaining

The rats were euthanized with 50 mg/ml phenobarbital at 72 h after HI ( $n=6$ /group) and at P47 ( $n=8$ /group). The animals were transcardially perfused with PBS followed by 4% paraformaldehyde in 0.1 M phosphate buffer (pH 7.4). The brains were removed and immersed sequentially in 20% sucrose solution (in 4% paraformaldehyde) then 30% sucrose solution in 0.1 M phosphate buffer (pH 7.4) until they sank. Coronal sections (30  $\mu$ m) were cut on a freezing microtome and stored in cryoprotectant solution at –20 °C.

Immunohistochemical studies were performed as previously described (Chen and Sun, 2007; Sheldon et al., 1996). Briefly, free-floating sections were washed with PBS three times and then incubated with 0.3% H<sub>2</sub>O<sub>2</sub> for 30 min. The sections were blocked with 0.3% goat serum and incubated overnight at 4 °C with the following primary antibodies: mouse anti-MBP (1:800, SMI-94R; Covance, Berkeley, CA, USA), GFAP (1:200, Ab-6; Neomarkers, Fremont, CA, USA), CD68 (1:500, Serotec-MCA341A; Kidlington, Oxford, UK), O4 (1:200, MAB345; Chemicon, International, CA, USA), CNPase (1:500, ab24566; Abcam, Cambridge, UK), and NeuN (1:500, MAB377; Chemicon, CA, USA). After rinsing, sections were incubated with goat anti-mouse IgG (1:200, BA-9200; Vector, Burlingame, CA, USA) or goat anti-mouse IgM (for O4, 1:200, M31515; Invitrogen, Camarillo, CA, USA) for 1 h and then incubated with an ABC kit (1:200, PK-6102;

Vector, Burlingame, CA, USA) for 1 h. The immunoreactivity was visualized with 0.05% diaminobenzidine chromogen. MBP immunostaining was evaluated at the bregma level in P47 rat brains as previously described (Fan et al., 2008a). Briefly, the image was captured by a charge-coupled device camera and the area of the corpus callosum, cingulum, and subcortical white matter was outlined with Image J software (public domain, National Institutes of Health, <http://rsbweb.nih.gov/ij/>).

### 4.3. Histologic evaluation

For histologic evaluations on P47, 30  $\mu$ m sections (1.60 to 4.80 mm from the bregma) of rats brain ( $n=15$  for HI and  $n=12$  for sham-operated control groups) were mounted on slides 360  $\mu$ m apart. The sections were stained with cresyl violet (Nissl; Sigma-Aldrich, St. Louis, MO, USA). Sections were rinsed briefly in PBS, dried overnight, and baked for 60 min at 37 °C. Sections were then rehydrated in decreasing concentrations of ethanol (100%, 95%, and 70%), stained with 3% cresyl violet solution for 3 min, dehydrated with increasing concentrations of ethanol (70%, 95%, and 100%), and cleared with xylene. The outlines of the corpus callosum and hemisphere were traced and the areas were measured by Image J software. The (R:L)<sub>AREA</sub> of the corpus callosum and hemisphere was calculated as the ratio of the ipsilateral area to the contralateral area or corresponding ipsilateral area to corresponding contralateral area in the HI group or control group, respectively. The sections at the level of the hippocampus (approximately –3.6 mm to the bregma) were selected for analysis of neuronal damage in the CA1 region.

### 4.4. Morris water maze test

The modified Morris water maze test was performed as previously described (Vorhees and Williams, 2006) on P42–P46 ( $n=23$  for HI and  $n=24$  for sham-operated control groups). For the navigation trial, four trials were performed daily for four consecutive days (14:00–16:00) for each rat. The pool was divided into four quadrants. A trial consisted of placing a rat into the water facing the wall of the pool at one of four starting positions, excluding the quadrant containing the platform. The platform was located in a constant position in the middle of the quadrant. During each block of four trials, each rat was placed in a random sequence of four starting positions. In each trial, the escape latency was recorded with a cutoff time of 120 s. If the animal located and climbed onto the platform within 120 s, a 15 s rest period occurred before the next trial. If the animal did not find the platform within 120 s, it was placed on the platform directly and allowed to rest for 15 s. The space probe trial was carried out at 14:00–16:00 on the 5th day (at P46). The platform was removed and both the number of platform crossings and the percentage of time spent in the target quadrant were recorded over a 30 s period. At the end of each trial, the rats were euthanized for immunostaining and determination of the (R:L)<sub>AREA</sub> ratios of the corpus callosum and hemisphere.

### 4.5. Data analysis

Because PWMI predominantly occurs in the periventricular area and subcortical white matter, sequential two sections of



these regions( approximately 1.2–0.6 mm to the bregma were analyzed at 400× magnification. The number of positive cells was counted at three consecutive high power fields (hpf; one view field=0.12 mm<sup>2</sup>) containing the cingulum and corpus callosum selectively, as previously described (Cai et al., 2006). The sections were evaluated by an examiner blinded to the treatment and the mean value of cell counting was used in one brain.

Data are presented as the mean ± S.E.M. Statistical comparisons of differences in O4-, CD68-, GFAP-, MBP-, CNPase-, NeuN-, and Nissl-positive cells were performed using one-way ANOVA followed by Student- Newman-Keuls test. A Student's t-test was performed to determine the differences in the number of platform crossings and percentage of time spent in the target quadrant. The Mann-Whitney *U* nonparametric test was performed to compare the (R:L)<sub>AREA</sub> ratios of the corpus callosum and cerebral hemispheres. A *p* value <0.05 was considered statistically significant.

## Acknowledgments

This work was sponsored by the Natural Science Foundation of China (Grant number 30772339. to Chao Chen).

The authors would like to thank Dr. Ben H Lee (Morristown, NJ, USA) for his assistance with manuscript preparation.

## REFERENCES

- Akiyama, K., Tanaka, R., Sato, M., Takeda, N., 2001. Cognitive dysfunction and histological findings in adult rats one year after whole brain irradiation. *Neurol. Med.-Chir.* 41, 590–598.
- Back, S.A., 2006. Perinatal white matter injury: the changing spectrum of pathology and emerging insights into pathogenetic mechanisms. *Ment. Retard. Dev. Disabil. Res. Rev.* 12, 129–140.
- Back, S.A., Volpe, J.J., 1997. Cellular and molecular pathogenesis of periventricular white matter injury. *Ment. Retard. Dev. Disabil. Res. Rev.* 3, 96–107.
- Back, S.A., Luo, N.L., Borenstein, N.S., Levine, J.M., Volpe, J.J., Kinney, H.C., 2001. Late oligodendrocyte progenitors coincide with the developmental window of vulnerability for human perinatal white matter injury. *J. Neurosci.* 21, 1302–1312.
- Back, S.A., Han, B.H., Luo, N.L., Chrifton, C.A., Xanthoudakis, S., Tam, J., Arvin, K.L., Holtzman, D.M., 2002. Selective vulnerability of late oligodendrocyte progenitors to hypoxia-ischemia. *J. Neurosci.* 22, 455–463.
- Cai, Z.W., Pang, Y., Xiao, F., Rhodes, P.G., 2001. Chronic ischemia preferentially causes white matter injury in the neonatal rat brain. *Brain Res.* 898, 126–135.
- Cai, Z., Lin, S., Fan, L.W., Pang, Y., Rhodes, P.G., 2006. Minocycline alleviates hypoxic-ischemic injury to developing oligodendrocytes in the neonatal rat brain. *Neuroscience* 137, 425–435.
- Chen, Y., Sun, F.Y., 2007. Age-related decrease of striatal neurogenesis is associated with apoptosis of neural precursors and newborn neurons in rat brain after ischemia. *Brain Res.* 1166, 9–19.
- Craig, A., Luo, N.L., Beardsley, D.J., Wingate-Pearse, N., Walker, D.W., Hohimer, A.R., Back, S.A., 2003. Quantitative analysis of perinatal rodent oligodendrocyte lineage progression and its correlation with human. *Exp. Neurol.* 181, 231–240.
- D'Hooge, R., De Deyn, P.P., 2001. Applications of the Morris water maze in the study of learning and memory. *Brain Res. Rev.* 36, 60–90.
- Di Giovanni, S., Movsesyan, V., Ahmed, F., Cernak, I., Schinelli, S., Stoica, B., Faden, A.I., 2005. Cell cycle inhibition provides neuroprotection and reduces glial proliferation and scar formation after traumatic brain injury. *Proc. Natl. Acad. Sci. U. S. A.* 102, 8333–8338.
- Dineen, R.A., Vilisaar, J., Hlinka, J., Bradshaw, C.M., Morgan, P.S., Constantinescu, C.S., Auer, D.P., 2009. Disconnection as a mechanism for cognitive dysfunction in multiple sclerosis. *Brain* 132, 239–249.
- Dwork, A.J., Mancevski, B., Rosoklija, G., 2007. White matter and cognitive function in schizophrenia. *Int. J. Neuropsychopharmacol.* 10, 513–536.
- Fan, L.W., Chen, R.F., Mitchell, H.J., Lin, R.C.S., Simpson, K.L., Rhodes, P.G., Cai, Z., 2008a. Alpha-Phenyl-*n*-tert-butyl-nitronne attenuates lipopolysaccharide-induced brain injury and improves neurological reflexes and early sensorimotor behavioral performance in juvenile rats. *J. Neurosci. Res.* 86, 3536–3547.
- Fan, L.W., Tien, L.T., Mitchell, H.J., Rhodes, P.G., Cai, Z.W., 2008b. Alpha-Phenyl-*n*-tert-butyl-nitronne ameliorates hippocampal injury and improves learning and memory in juvenile rats following neonatal exposure to lipopolysaccharide. *Eur. J. Neurosci.* 27, 1475–1484.
- Fawcett, J.W., Asher, R.A., 1999. The glial scar and central nervous system repair. *Brain Res. Bull.* 49, 377–391.
- Fields, R.D., 2005. Myelination: an overlooked mechanism of synaptic plasticity? *Neuroscientist* 11, 528–531.
- Fields, R.D., 2008a. White matter matters. *Sci. Am.* 298, 54–61.
- Fields, R.D., 2008b. White matter in learning, cognition and psychiatric disorders. *Trends Neurosci.* 31, 361–370.
- Follett, P.L., Rosenberg, P.A., Volpe, J.J., Jensen, F.E., 2000. NBQX attenuates excitotoxic injury in developing white matter. *J. Neurosci.* 20, 9235–9241.
- Franklin, R.J.M., Ffrench-Constant, C., 2008. Remyelination in the CNS: from biology to therapy. *Nat. Rev., Neurosci.* 9, 839–855.
- Inder, T.E., Warfield, S.K., Wang, H., Huppi, P.S., Volpe, J.J., 2005. Abnormal cerebral structure is present at term in premature infants. *Pediatrics* 115, 286–294.
- Juraska, J.M., Kopcik, J.R., 1988. Sex and environmental-influences on the size and ultrastructure of the rat corpus-callosum. *Brain Res.* 450, 1–8.
- Kujala, P., Portin, R., Ruutiainen, J., 1997. The progress of cognitive decline in multiple sclerosis—a controlled 3-year follow-up. *Brain* 120, 289–297.
- Lin, S.Y., Rhodes, P.G., Lei, M.P., Zhang, F., Cai, Z.W., 2004. Alpha-Phenyl-*n*-tert-butyl-nitronne attenuates hypoxic-ischemic white matter injury in the neonatal rat brain. *Brain Res.* 1007, 132–141.
- Lin, S., Fan, L.W., Pang, Y., Rhodes, P.G., Mitchell, H.J., Cai, Z., 2005. IGF-1 protects oligodendrocyte progenitor cells and improves neurological functions following cerebral hypoxia-ischemia in the neonatal rat. *Brain Res.* 1063, 15–26.
- Liu, Y., Silverstein, F.S., Skoff, R., Barks, J.D., 2002. Hypoxic-ischemic oligodendroglial injury in neonatal rat brain. *Pediatr. Res.* 51, 25–33.
- Marlow, N., Wolke, D., Bracewell, M.A., Samara, M., 2005. Neurologic and developmental disability at six years of age after extremely preterm birth. *N. Eng. J. Med.* 352, 9–19.
- Menn, B., Garcia-Verdugo, J.M., Yaschine, C., Gonzalez-Perez, O., Rowitch, D., Alvarez-Buylla, A., 2006. Origin of oligodendrocytes in the subventricular zone of the adult brain. *J. Neurosci.* 26, 7907–7918.
- Miki, K., Ishibashi, S., Sun, L.Y., Xu, H.Y., Ohashi, W., Kuroiwa, T., Mizusawa, H., 2009. Intensity of chronic cerebral hypoperfusion determines white/gray matter injury and cognitive/motor dysfunction in mice. *J. Neurosci. Res.* 87, 1270–1281.

- Ohta, H., Nishikawa, H., Kimura, H., Anayama, H., Miyamoto, M., 1997. Chronic cerebral hypoperfusion by permanent internal carotid ligation produces learning impairment without brain damage in rats. *Neuroscience* 79, 1039–1050.
- Pierson, C.R., Folkerth, R.D., Billiards, S.S., Trachtenberg, F.L., Drinkwater, M.E., Volpe, J.J., Kinney, H.C., 2007. Gray matter injury associated with periventricular leukomalacia in the premature infant. *Acta Neuropathol.* 114, 619–631.
- Sanchez, M.M., Hearn, E.F., Do, D., Rilling, J.K., Herndon, J.G., 1998. Differential rearing affects corpus callosum size and cognitive function of rhesus monkeys. *Brain Res.* 812, 38–49.
- Segovia, K.N., McClure, M., Moravec, M., Luo, N.L., Wan, Y., Gong, X., Riddle, A., Craig, A., Struve, J., Sherman, L.S., Back, S.A., 2008. Arrested oligodendrocyte lineage maturation in chronic perinatal white matter injury. *Ann. Neurol.* 63, 520–530.
- Sheldon, R.A., Chuai, J., Ferriero, D.M., 1996. A rat model for hypoxic-ischemic brain damage in very premature infants. *Biol. Neonate* 69, 327–341.
- Sizonenko, S.V., Camm, E.J., Dayer, A., Kiss, J.Z., 2008. Glial responses to neonatal hypoxic-ischemic injury in the rat cerebral cortex. *Int. J. Dev. Neurosci.* 26, 37–45.
- Skoff, R.P., Bessert, D.A., Barks, J.D., Song, D., Cerghet, M., Silverstein, F.S., 2001. Hypoxic-ischemic injury results in acute disruption of myelin gene expression and death of oligodendroglial precursors in neonatal mice. *Int. J. Dev. Neurosci.* 19, 197–208.
- Stone, B.S., Zhang, J.Y., Mack, D.W., Mori, S., Martin, L.J., Northington, F.J., 2008. Delayed Neural Network Degeneration after Neonatal Hypoxia-Ischemia. *Ann. Neurol.* 64, 535–546.
- Taylor, H.G., Minich, N., Bangert, B., Filpek, P.A., Hack, M., 2004. Long-term neuropsychological outcomes of very low birth weight: associations with early risks for periventricular brain insults. *J. Int. Neuropsychol. Soc.* 10, 987–1004.
- Ten, V.S., Bradley-Moore, M., Gingrich, J.A., Stark, R.I., Pinsky, D.J., 2003. Brain injury and neurofunctional deficit in neonatal mice with hypoxic-ischemic encephalopathy. *Behav. Brain Res.* 145, 209–219.
- Vannucci, R.C., Connor, J.R., Mauer, D.T., Palmer, C., Smith, M.B., Towfighi, J., Vannucci, S.J., 1999. Rat model of perinatal hypoxic-ischemic brain damage. *J. Neurosci. Res.* 55, 158–163.
- Volpe, J.J., 2001. Neurobiology of periventricular leukomalacia in the premature infant. *Pediatr. Res.* 50, 553–562.
- Vorhees, C.V., Williams, M.T., 2006. Morris water maze: procedures for assessing spatial and related forms of learning and memory. *Nat. Protoc.* 1, 848–858.
- Zhu, C., Wang, X., Huang, Z., Qiu, L., Xu, F., Vahsen, N., Nilsson, M., Eriksson, P.S., Hagberg, H., Culmsee, C., Plesnila, N., Kroemer, G., Blomgren, K., 2007a. Apoptosis-inducing factor is a major contributor to neuronal loss induced by neonatal cerebral hypoxia-ischemia. *Cell Death Differ.* 14, 775–784.
- Zhu, Z., Zhang, Q., Yu, Z., Zhang, L., Tian, D., Zhu, S., Bu, B., Xie, M., Wang, W., 2007b. Inhibiting cell cycle progression reduces reactive astrogliosis initiated by scratch injury in vitro and by cerebral ischemia in vivo. *Glia* 55, 546–558.